特集

# Compact and Tunable Transmitter and Receiver for Magnetic Resonance Power Transmission to Mobile Objects*

Takashi KOMARU　Masayoshi KOIZUMI　Kimiya KOMURASAKI
Takayuki SHIBATA and Kazuhiko KANO

This paper discusses the feasibility of wireless power transmission with magnetic resonance to mobile objects. The theoretical analysis on magnetic resonance showed that efficient wireless power transmissions need high quality factor resonators and impedance matching systems. In addition to those elements, mobile applications need compact and tunable transmitters and receivers because impedance matching conditions change according to varying transmission distances. We developed an experimental transmitter and receiver. They consist of resonator and pickup loop both made with a single-turn copper wire loop and a lumped capacitor. The resonator and the pickup loop are placed in parallel and very close to each other. This structure makes the transmitter and receiver axially compact. And the position adjustable pickup loop enables the impedance matching in tune with varying transmission distances. This system showed high transmission efficiencies as predicted from the theoretical analysis.

**Key words** : Wireless power, magnetic resonance, quality factor, impedance matching

電子要素

## 1. Introduction

As electronic devices are becoming more mobile and ubiquitous, power cables are turning to the bottlenecks in the full-fledged utilization of electronics. While battery capacities are reaching their limits, wireless power transmission with magnetic resonance is expected to provide a breakthrough for this situation by enabling power feeding available anywhere and anytime.

This chapter studies the feasibility of magnetic resonance power transmission to mobile objects mainly focusing on the resonator quality factor and impedance matching control systems. Transmission efficiency reaches a reasonably high level when the transmitting and receiving resonators satisfy two conditions. The first is to have high quality factors. The second is to tune and match the impedance to the transmission distances. The second section explains the theoretical grounds for these conditions. The third section describes a developed wireless power transmission system prototype which was made compact and tunable to be applied to mobile objects. The later sections evaluate the quality factor and the impedance matching of the prototype.

## 2. Theoretical analysis of a magnetic resonance system

This section states the theoretical basics of wireless power transmission with magnetic resonance. The theory is developed by using the logic of electrical engineering without the coupled-mode theory. First, the base concept of a wireless power transmission system and its equivalent circuit model are introduced. Then the transmission efficiency is derived as a formula with the physical properties including the impedances and the mutual inductance. This formula is simplified by replacing the physical properties with the non-dimensional parameters including impedance ratio, quality factor and coupling coefficient. Analysis of this simplified formula derives the essential principle for efficient mid-range wireless power transmission.

### 2.1 Basic model

The model of a wireless power transmission system with magnetic resonance is expressed as per **Fig. 1(a)** and **Fig. 1(b)**. Two resonators of a series LCR (inductor, capacitor and resister) are inductively coupled to each other. Note that this model also applies to the basic system of wireless power transmission with electromagnetic induction. The currents flowing through the source and load are derived from Kirchhoff's second law as per (1).

* Reprinted from "Wireless Power Transfer - Principles and Engineering Explorations", ISBN: 978-953-307-874-8, InTech according to the terms set by InTech's Copyright Policy

$$\begin{bmatrix} V_{src} \\ 0 \end{bmatrix} = \begin{bmatrix} Z_S & j\omega M_{SD} \\ j\omega M_{SD} & Z_D + Z_{0ld} \end{bmatrix} \begin{bmatrix} I_{src} \\ I_{ld} \end{bmatrix}$$

$$\Rightarrow \begin{bmatrix} I_{src} \\ I_{ld} \end{bmatrix} = \frac{V_{src}}{Z_S(Z_D + Z_{0ld}) + (\omega M_{SD})^2} \begin{bmatrix} Z_D + Z_{0ld} \\ -j\omega M_{SD} \end{bmatrix} \quad (1)$$

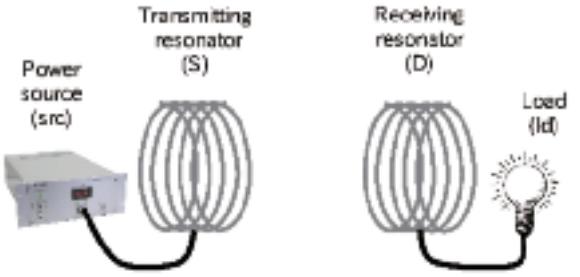


(a) Image of the basic system

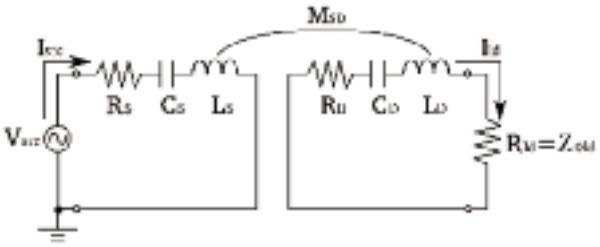


(b) Equivalent circuit model

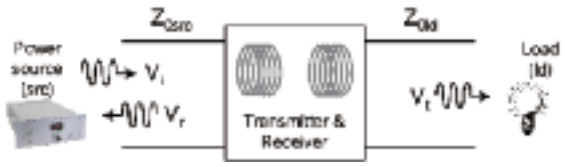


(c) Two-port network unit model

Fig. 1　Three types of concept figures of the basic wireless power transmission system model

Note that ω represents the angular frequency. Voltage $V_{src}$ and currents $I_{src}$, $I_{ld}$ are in phasor form and are complex properties. Impedance $Z_S$ is defined as the impedance of the transmitting resonator $R_S + j(\omega L_S - 1/\omega C_S)$. Impedance $Z_D$ is also defined in the same way as $Z_S$. $Z_{0src}$ represents the characteristic impedance of the transmission line in the power source device and the cable between the source and transmitting resonator. Impedance $Z_{0ld}$ represents the characteristic impedance of the transmission line in the cable between the load and receiving resonator. These characteristic impedances are assumed to be a real number. The load resistance $R_{ld}$ is matched to $Z_{0ld}$ so that the load absorbs all transmitted power and reflects no power to the receiving resonator.

Since the source frequency is often set to a high value of about 10 MHz, the concepts of incident wave, reflected wave and transmitted wave should be introduced [4]. As **Fig. 1(c)** shows, the coupled resonators inserted between the source and the load can be considered as a two-port network unit. This unit receives incident waves from the source. At the same time, it produces reflected waves to the source and transmitted waves to the load. Voltage $V_i$, $V_r$ and $V_t$ represent the amplitude of each wave respectively. And they are expressed by the properties of the circuit model as per (2).

$$V_i = \frac{V_{src} + Z_{0src} I_{src}}{2}, V_r = \frac{V_{src} - Z_{0src} I_{src}}{2}, V_t = Z_{0ld} I_{ld} \quad (2)$$

The power of each wave is as per (3).

$$P_i = \frac{|V_i|^2}{2Z_{0src}}, P_r = \frac{|V_r|^2}{2Z_{0src}}, P_t = \frac{|V_t|^2}{2Z_{0ld}} \quad (3)$$

Then the transmission efficiency is defined as the ratio of transmitted wave power and incident wave power.

$$\eta = \frac{P_t}{P_i} = \frac{4Z_{0src}Z_{0ld}(\omega M_{SD})^2}{|(Z_S + Z_{0src})(Z_D + Z_{0ld}) + (\omega M_{SD})^2|^2} \quad (4)$$

The reflection efficiency is also defined as the ratio of reflected wave power and incident wave power.

$$\eta = \frac{P_r}{P_i} = \left| \frac{(Z_S - Z_{0src})(Z_D + Z_{0ld}) + (\omega M_{SD})^2}{(Z_S + Z_{0src})(Z_D + Z_{0ld}) + (\omega M_{SD})^2} \right|^2 \quad (5)$$

Equation (4) is the fundamental definition of efficiency. However, in some cases such as low frequency operations, the power source can reuse the reflected wave. Then the transmission efficiency becomes $\eta' = \eta/(1-\eta_r)$, which is equal to the efficiency derived from a simple AC circuit calculation as per (6). Note that θ represents the phase difference between $V_{src}$ and $I_{src}$.

$$\eta' = \frac{\eta}{1-\eta_r} = \frac{Z_{0ld}|I_{ld}|^2}{|V_{src}I_{src}|\cos\theta} = \frac{Z_{0ld}|I_{ld}|^2}{R_S|I_{src}|^2 + (R_D + Z_{0ld})|I_{ld}|^2} \quad (6)$$

### 2.2　Analysis of transmission efficiency

The following non-dimensional parameters are useful when considering the transmission efficiency analytically.

- Coupling coefficient $k = M_{SD}/(L_S L_D)^{1/2}$
- Quality factor $Q_S = \omega_0 L_S/R_S$ and $Q_D = \omega_0 L_D/R_D$
- Impedance ratio $r_S = Z_{0src}/R_S$ and $r_D = Z_{0ld}/R_D$

Note that the resonant frequencies are assumed to be equal to each other ($(LsCs)^{-1/2} = (LDCD)^{-1/2} = \omega 0$) for simplicity in this discussion. The frequency band is considered narrow enough ($|\omega - \omega 0| << \omega 0$). Then (4) is expressed as (7) by using the approximations $\omega/\omega 0 - \omega 0/\omega \approx 2(\omega - \omega 0)/\omega 0$ and $\omega \approx \omega 0$.

$$\eta = \frac{4k^2 \frac{r_S}{Q_S}\frac{r_D}{Q_D}}{\left[k^2 - \alpha\left(\frac{\omega-\omega_0}{\omega_0}\right)^2 + \frac{1+r_S}{Q_S}\frac{1+r_D}{Q_D}\right]^2 + \alpha\left(\frac{\omega-\omega_0}{\omega_0}\right)^2\left(\frac{1+r_S}{Q_S}+\frac{1+r_D}{Q_D}\right)^2} \quad (7)$$

Efficiency η' is also expressed by the non-dimensional parameters.

$$\eta' = \frac{k^2 Q_S Q_D}{(1+r_D)(1+r_D+k^2 Q_S Q_D)+[4(\omega-\omega_0)/\omega]^2 Q_D^2} \quad (8)$$

In the $\omega - rS - rD$ domain, η has its maximum value (9) at (10).

$$\eta_{max} = \frac{k^2 Q_S Q_D}{\left(1+\sqrt{1+k^2 Q_S Q_D}\right)^2} \quad (9)$$

$$\omega = \omega_0, r_S = r_D = \sqrt{1+k^2 Q_S Q_D} \quad (10)$$

The physical meaning of (10) is the impedance matching condition. In the case $rS = rD$, η in the $\omega - rS - rD$ domain becomes visible as the surface in **Fig. 2**, which clearly shows the existence of a maximum point. It is not easy to prove directly from (7) that (9) is exactly the maximum. However, there is a simple and strict proof via analysis at (8).

$$\eta' \le \frac{k^2 Q_S Q_D r_D}{(1+r_D)(1+r_D+k^2 Q_S Q_D)} \quad (11)$$

$$\le \frac{k^2 Q_S Q_D}{(1+k^2 Q_S Q_D)^2} = \eta_{max} \quad (12)$$

The equality in (11) and (12) is approved when $\omega = \omega 0$ and $rD = (1 + k^2 QSQD)^{1/2}$ respectively. These directly mean the maximum of η' is $\eta'_{max} = \eta_{max}$ at $\omega = \omega 0$ and $rD = (1 + k^2 QSQD)^{1/2}$. Besides $\eta \le \eta'$ because $\eta' \le \eta/(1 - \eta r)$ and $0 \le \eta r \le 1$. Thus the maximum value of (7) is proved to be (9) as per (13).

$$\eta \le \eta' \le \eta'_{max} \Rightarrow \eta \le \eta_{max} \quad (13)$$

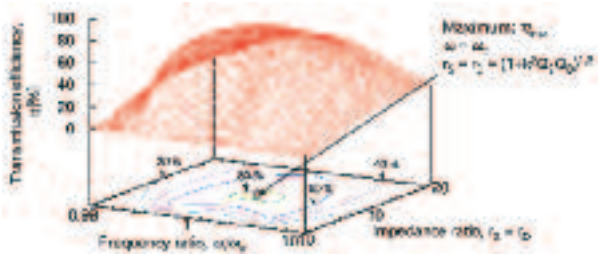


Fig. 2　Three dimensional plot and contour of the transmission efficiency in $\omega - r$ domain with $k = 0.01$ and $QS = QD = 1000$.

Equation formula (9) depends only on one term $k(QSQD)^{1/2}$ and draws a simple curve as shown in **Fig. 3**.

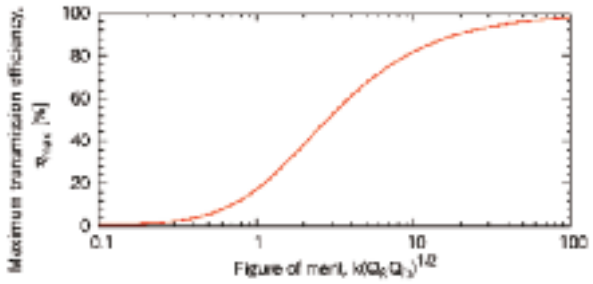


Fig. 3　Maximum transmission efficiency plotted along figure-of-merit

Here the principles for efficient power transmission are derived without referring to the coupled-mode theory.

- $k(QSQD)^{1/2}$ is defined as figure-of-merit (*fom*).
- Impedance ratio should be matched to $(1 + fom^2)^{1/2}$.
- Figure-of-merit in 1 or higher order enables efficient wireless power transmission with over 20 % efficiency. (The concept of a strong coupling regime.)

They completely correspond to the characteristics of mid-range transmission argued in the original theory of magnetic resonance [1]. In fact, $k(QSQD)^{1/2}$ can be derived from the original expression of figure-of-merit $\varkappa/(\Gamma s \Gamma D)^{1/2}$ [2]. In the field of electrical engineering, coupling coefficient $k$ and the quality factor $Q$ are more intuitive parameters than the reciprocally-time-dimensional coupling coefficient $\varkappa$ and decay constant $\Gamma$. Thus the redefinition of figure-of-merit helps the understanding of mid-range transmission in comparison with conventional close-range electromagnetic inductance. In close-range electromagnetic inductance, $k$ is over 0.8 in most cases and rarely less than 0.2. Therefore, it is relatively easy to achieve high transmission efficiency of over 80 % [6) 8)]. Meanwhile in the mid-range, the transmission distance is equal to or greater than the size of resonators and $k$ becomes a very low value of $10^2$ or lower

order. Here, the principle of the strong coupling regime concept leads to the point of importance : it is a high quality factor of $10^2$ or greater order that enables efficient transmission even with very low $k$ in mid-range.

In addition to high quality factor, impedance matching is needed for efficient transmission in mid-range. Mid-range wireless power transmission is expected to bring much more flexibility in receiver and transmitter positioning than close range wireless power transmission. And this means the coupling coefficient between transmitting and receiving resonators can take various values. Moreover in mobile applications, receivers and transmitters will be equipped on moving objects and have to exchange power across ever-changing transmission distance and coupling coefficients. As stated before, the impedance ratio $r_S$ and $r_D$ must be matched to $(1 + fom^2)^{1/2} = (1 + k^2 Q_S Q_D)^{1/2}$ in order to obtain the highest efficiency. **Fig. 4** shows how transmission efficiency changes with different coupling coefficients. When the receiver comes to the closer (a) or the farther (c) position than the original position (b), coupling coefficient becomes larger or smaller and the maximum point in ω-r domain changes to the higher-$r$ or the lower-$r$ point. Thus we must consider a system that controls the impedance ratio according to the variable transmission distance.

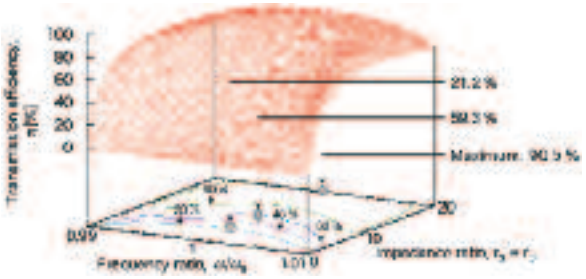

(a) $k$ =0.02

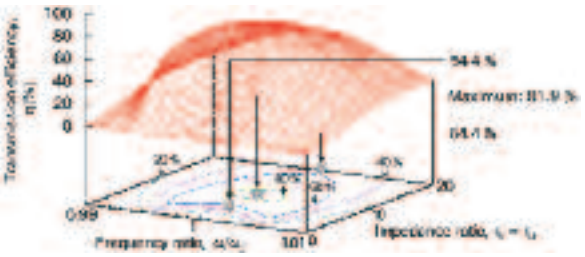

(b) $k$ =0.01

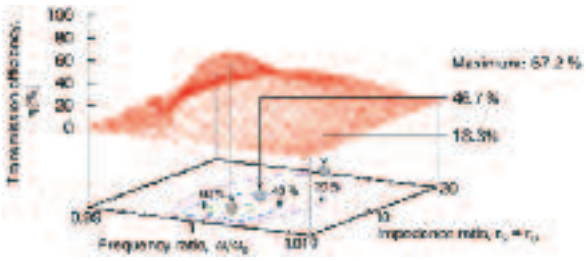

(c) $k$ =0.005

Fig. 4　Three dimensional plot and contour of transmission efficiencies in $\omega - r$ domain with various coupling coefficients $k$ and quality factors $Q_S = Q_D = 1000$

There are three schemes considered for the impedance matching control : two-sided, one-sided and no control. In the two-sided control scheme, both the transmitter and the receiver take the optimum impedance ratios. In the one-sided control scheme, either the transmitter or the receiver takes the optimum one and the other takes a fixed one. In the no control scheme, both the transmitter and the receiver take fixed ones. The theoretical efficiencies with these control schemes are expressed as follows :

$$\eta_2 = \frac{k^2 Q_S Q_D}{\left(1 + \sqrt{1 + k^2 Q_S Q_D}\right)^2} \tag{14}$$

$$\eta_1 = \frac{k^2 Q_S Q_D r_D}{(1 + r_D)(1 + r_D + k^2 Q_S Q_D)} \tag{15}$$

$$\eta_0 = \frac{4k^2 Q_S Q_D r_S r_D}{[(1 + r_S)(1 + r_D) + k^2 Q_S Q_D]^2} \tag{16}$$

Note that $\eta_2$, $\eta_1$ and $\eta_0$ represent the efficiency with two-sided, one-sided and no control scheme respectively. Equation 15 assumes that the transmitter has the optimized impedance ratio and the receiver has the fixed one. When the transmitter has the fixed one and the receiver has the optimized one in reverse, $r_D$ and $r_S$ switch positions with each other. The no control efficiency $\eta_0$ is derived from $\eta$ in (7) by substituting $\omega$ with $\omega_0$. The one-sided control efficiency $\eta_1$ is derived from the partial differential analysis of $\eta_0$ as follows.

$$\frac{\partial}{\partial r_S} \log \eta_0 = 0 \Rightarrow k^2 Q_S Q_D + (1 - r_S)(1 - r_D) = 0 \tag{17}$$

Efficiency $\eta_1$ is equal to $\eta'$ in (8) with $\omega = \omega_0$. This means the reuse of the reflected power by the power source is equal

to the optimization of the transmitter impedance ratio. The two-sided control efficiency $\eta_2$ is exactly the same as $\eta_{max}$.

The characteristics of the transmission efficiencies for the two-sided, one-sided and no control are visualized by **Fig. 5**. Generally, two-sided control always takes the maximum efficiency, while it will take more hardware and software cost for the control system. No control will only need a simple and low-cost system in exchange for efficiency at various transmission distances. One-sided control has the middle characteristics.

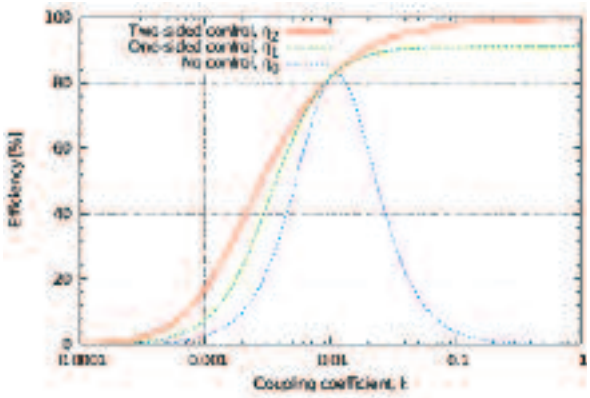


Fig. 5　Transmission efficiency with the three types of impedance matching control schemes. The quality factors are $Q_S = Q_D = 1000$. The impedance ratios are fixed as $r_S = [1 + (10^{-2})^2 Q_S Q_D]^{1/2}$ in the one-sided control and $r_S = r_D = [1 + (10^{-2})^2 Q_S Q_D]^{1/2}$ in the no control.

## 3. Specifications of the transmitter and the receiver

Efficient mid-range wireless power transmission with magnetic resonance needs a high quality factor resonator and impedance matching system. Mobile object applications need compact and tunable transmitters and receivers. We developed an experimental transmitter and receiver system that satisfy those conditions as shown in **Fig. 6**. The system consists of a resonator and a pickup loop. The resonator is a copper wire loop with a lumped mica capacitor. The pickup loop is also a copper wire loop with a lumped mica capacitor. The combination of the resonator and the pickup loop function as an inductive transformer, which virtually transforms the characteristic impedance of the source and the load. Both the resonator and the wire loop have only a single turn and they are placed in parallel and very close to each other. This structure makes the transmitter and receiver axially compact. Note that the resonant frequencies of the resonator and the pickup loop are designed to be equal to each other. The following two sections state the performance analyses of the system.

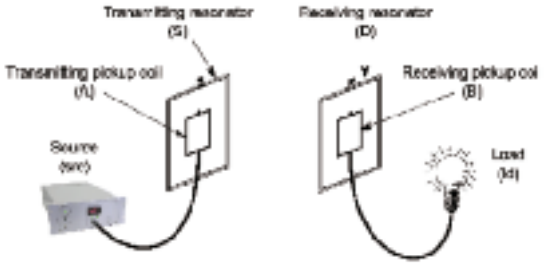


(a) Overall view of the power transmission system

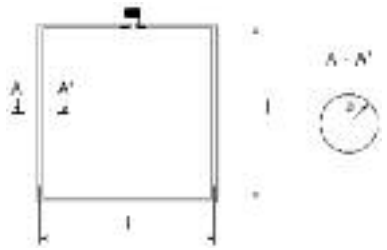


(b) The resonator with side length $\ell \times \ell = 198$ mm × 198 mm, wire radius $a = 1.5$ mm and capacitor capacitance : $C = 200$ pF.

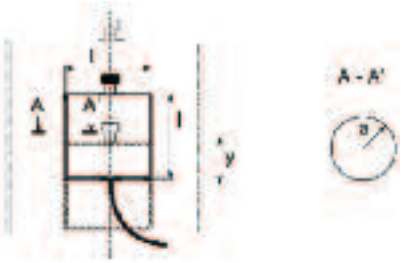


(c) The pickup loop with side length $\ell \times \ell = 92$ mm × 92 mm, wire radius $a = 1.0$ mm, capacitor capacitance $C = 470$ pF and sliding position $y = 0$ - 48 mm.

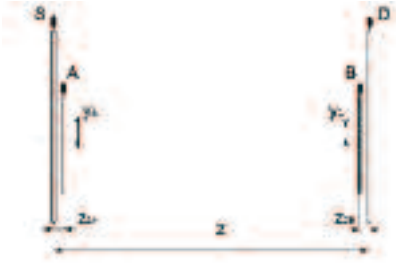


(d) Alignment of the resonators and pickup loops with the pick-up loop slide positions $y_S$, $y_D = 0$ - 48 mm and the spaces between resonator and pickup loop $Z_{SA} = Z_{DB} = 2.0$ mm.

Fig. 6　Transmitter and receiver specification

## 4. Resonator quality factor

Resonators may take any shape and any materials. A popular type of resonator is a coil with multiple turns. To make it compact, the turn pitch has to be as small as possible. But with such a dense coil structure, it is hard to have high quality factor because of the electricity loss due to the insulating cover on the wire [7]. The other widely considered type is a coil with a single turn and a lumped capacitor. In this study, we call this type "loop with capacitor" and analyze it as a primary model of the resonator.

### 4.1 Theoretical calculation

An exact calculation of quality factors is indispensable to design and evaluate the wireless power transmission system with magnetic resonance. As stated in the previous section, a resonator is equivalent to a series LCR element and quality factor Q is generally derived as the ratio of resonant frequency $f_0 = \omega_0/2\pi = 1/2\pi(LC)^{1/2}$, self-inductance $L$ and resistance $R$ of a resonator.

$$Q = \frac{\omega_0 L}{R} \tag{18}$$

Of these properties, resistance is the most difficult to calculate regarding its realizable value. The predictions in most conventional research only take account of two types of resistance : radiation and ohmic resistance. This chapter also calculates capacitor resistance to predict the quality factor precisely. Then the properties to be calculated are resonant frequency, self-inductance, radiation resistance ohmic resistance and capacitor resistance. The first four properties are calculated by the theoretical equations derived from the electromagnetism. The other capacitor resistance is estimated by using the measured specification data of a capacitor element.

The total length of the resonator wire is about 0.8m and is far smaller than the wavelength of about 30m in the supposed frequency band. Thus the current distribution on the wire is approximated to be uniform hereinafter.

For a rectangle loop with a side length $\ell x$, $\ell y$ and a wire radius $a$, the self-inductance is expressed as (19) [5].

$$L = \frac{\mu_0}{\pi}\left[\ell_x \ln\left(\frac{2\ell_x}{a}\right) + \ell_y \ln\left(\frac{2\ell_y}{a}\right) + 2\sqrt{\ell_x^2 + \ell_y^2} - \ell_x \sinh^{-1}\left(\frac{\ell_x}{\ell_y}\right) - \ell_y \sinh^{-1}\left(\frac{\ell_y}{\ell_x}\right) - 1.75(\ell_x + \ell_y)\right] \tag{19}$$

Substituting $\ell x$ and $\ell y$ with $\ell$ leads to

$$L = \frac{2\mu_0 \ell}{\pi}\left[\ln\left(\frac{2\ell}{a}\right) - 1.2172\right] \tag{20}$$

The uniform current distribution means zero electrical charge density at every point on the wire. Therefore the resonator capacitance originates just from the lumped capacitor. Then the resonant frequency is

$$\omega_0 = 1/\sqrt{LC} \tag{21}$$

The resonator is approximated as a small current loop, which is theoretically equal to a small magnetic dipole as in **Fig. 7**, because of the loop size being far smaller than the wavelength. The radiation resistance is derived from consideration of this small magnetic dipole model. A small electrical dipole with current $I$ and length $dz$ radiates power expressed as

$$\frac{\pi |I|^2}{3}\sqrt{\frac{\mu_0}{\epsilon_0}}\left(\frac{dz'}{\lambda_0}\right)^2 \tag{22}$$

Note that $\lambda_0$ is the vacuum wavelength $c_0/f_0 = 2\pi c_0/\omega_0$. According to the symmetry of Maxwell's equations, $\epsilon_0$, $\mu_0$ and $I$ are the dual of $\mu_0$, $\epsilon_0$ and $I_m$ respectively. $I_m$ represents the magnetic current [3]. Then the radiated power from a small magnetic dipole is expressed as

$$P_{rad} = \frac{\pi |I_m|^2}{3}\sqrt{\frac{\epsilon_0}{\mu_0}}\left(\frac{dz'}{\lambda_0}\right)^2 \tag{23}$$

From the definition of the magnetic dipole moment of both the magnetic dipole and the electrical current loop

$$Q_m dz' = \mu_0 I dS' \tag{24}$$

where $dS'$ is the loop area corresponding to $\ell^2$ and $Q_m$ is the magnetic charge with the relation

$$I_m = \frac{\partial Q_m}{\partial t} = j\omega Q_m \tag{25}$$

The radiated power is then transformed to

$$P_{rad} = \frac{\mu_0 \omega^4 \ell^4}{12\pi c_0^3} |I|^2 \tag{26}$$

which should be equal to

$$P_{rad} = \frac{1}{2} R_{rad} |I|^2 \tag{27}$$

Hence the radiation resistance is

$$R_{rad} = \frac{\mu_0 \omega^4 \ell^4}{6\pi c_0^3} \tag{28}$$


Fig. 7　Magnetic dipole and electrical current loop

The basic expression of the ohmic resistance for a wire with conductivity σ, sectional area $S$ and length $d\ell$ is

$$R_{ohm} = \frac{d\ell}{\sigma S} \tag{29}$$

When the frequency is high, current density decays exponentially along the depth from the surface to the center of the wire. The skin depth δs is defined as the inverse of the decay constant [4] as

$$\delta_s = \sqrt{\frac{2}{\omega\mu\sigma}} \tag{30}$$

and wire sectional area $S$ in (29) is substituted with $S = 2\pi a\delta s$

$$R_{ohm} = \frac{d\ell}{2\pi a}\sqrt{\frac{\mu\omega}{2\sigma}} \tag{31}$$

the total wire length of the resonator is $4\ell$ and the ohmic resistance finally becomes

$$R_{ohm} = \frac{\ell}{\pi a}\sqrt{\frac{2\mu\omega}{\sigma}} \tag{32}$$

A real capacitor is not a pure capacitive element but a complex component with various impedance elements. In the frequency band of wireless power transmission, the dominant characteristics are the original capacitance and the equivalent series resistance (ESR). This study calls ESR “capacitor resistance” and analyzes its value. The characteristics of the actual capacitor were measured by the LCR meter. The meter gave the loss coefficient data as in **Fig. 8**. Note that the approximated line is derived by using the least-squares method. The loss coefficient of the capacitor is defined as

$$D(\omega) = -\frac{R(\omega)}{X(\omega)} = \omega CR \tag{33}$$

Note that $X$ and $R$ here represent the reactance and the resistance of the capacitor respectively. The capacitor resistance is then expressed as

$$R_{cap} = \frac{D(\omega)}{\omega C} \tag{34}$$

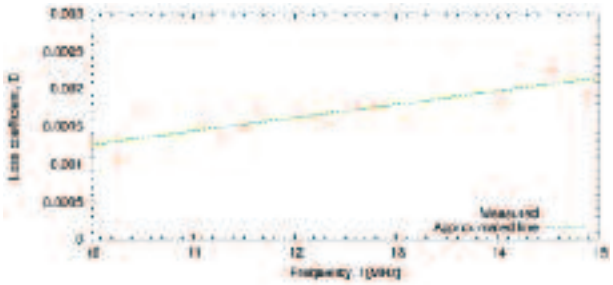

Fig. 8　Characteristics of the capacitor loss coefficient

### 4.2　Experimental measurement

The comparison with the calculated and the measured quality factors are shown in **Fig. 9** in the form of the loss coefficient. Note that the loss coefficient is the inverse of the quality factor. The calculated loss coefficient is classified into the three categories corresponding to the three resistances introduced in the previous subsection. The radiation loss is too small to be visible in this graph. The predicted resonant frequencies and the quality factors are well agreed with the measured parameters, verifying the calculation method stated in this section. The important point is the quality factor of the loop with the capacitor type resonator was higher than that of the dense coil type resonator at about $Q = 200$ as measured in our previous study. And the capaci-

tor loss was as large as the ohmic loss. This means that the calculation of the capacitor loss was indispensable. Note that the measured resonant frequencies of the transmitting and the receiving resonator were 13.43 and 13.46 MHz. They also agreed with the calculated value of 13.54 MHz.

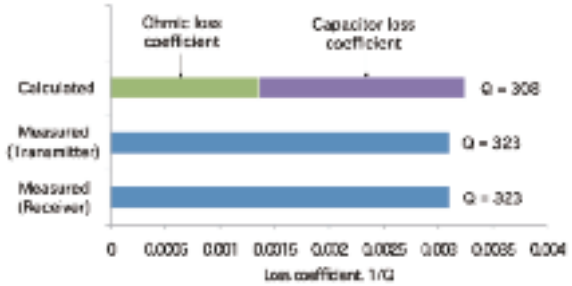


Fig. 9　Comparison between the calculated and the measured quality factors

## 5.　Impedance matching control system

Impedance matching means the transformation of the source and the load impedance. The impedance matching system has the same purpose as the antenna tuners. There are several ways to implement impedance matching : some use a set of variable capacitors and inductors and some others use transistors for example. The main requirement of the impedance matching system for efficient transmission is low electrical loss. And for mobile applications, it is also required to be compact and have wide range of impedance transformation. This chapter considers a sliding pickup loop system as a simple and compact transmitter and receiver prototype.

### 5.1　Basics of impedance matching with pickup loop

Impedance transformation is explained as follows. The coupling of the resonator and the pickup loop is equivalent to the circuit model shown in **Fig. 10**. Though the indices here are for the receiving resonator and the pickup loop, the same result is obtained for the transmitting resonator and the pickup loop. And the following mutual inductances are assumed to be negligible: $M_{AB}$ between the transmitting and the receiving pickup loop, $M_{SB}$ between the transmitting resonator and the receiving pickup loop and $M_{DA}$ between the receiving resonator and the transmitting pickup loop. From Kirchhoff's second law for the circuit, the currents flowing in the resonator and the pickup loop $I_D$, $I_{Id}$ is expressed by the voltage in the resonator $V$ which the current in the pickup loop inducted.

$$\begin{bmatrix} V \\ 0 \end{bmatrix} = \begin{bmatrix} 0 & j\omega M_{DB} \\ j\omega M_{DB} & Z_B + Z_{Old} \end{bmatrix} \begin{bmatrix} I_D \\ I_{Id} \end{bmatrix}$$
$$\Rightarrow \begin{bmatrix} I_D \\ I_{Id} \end{bmatrix} = \frac{V}{(\omega M_{DB})^2} \begin{bmatrix} Z_B + Z_{Old} \\ -j\omega M_{DB} \end{bmatrix} \quad (35)$$

Then the pickup loop and the load that are inductively coupled to the resonator equal to the impedance $Z_{Old}$ directly connected to the resonator.

$$Z'_{Old} = \frac{V}{I_D} = \frac{(\omega M_{DB})^2}{Z_B + Z_{Old}} \quad (36)$$

Note that $Z_B$ represents the impedance of the pickup loop $Z_B = R_B + j\,(\omega L_B - 1/\omega C_B)$. Let the resonant frequency of the pickup loop equal the resonant frequency of the resonator and the source frequency so that the pickup loop reactance is zero $Z_B = R_B$. Now the impedance ratio becomes

$$r_D = \frac{Z'_{Old}}{R_D} = \frac{V}{R_D I_D} = \frac{(\omega M_{DB})^2}{R_D (R_d + Z_{Old})} \quad (37)$$

This is the function of the mutual inductance between the resonator and the pickup loop. This means it is possible to control the impedance ratio by changing the coupling condition, including the relative position, of the resonator and the pickup loop.

To design a transmitter or a receiver with this pickup loop impedance matching system and acquire the desired impedance ratios, the following properties have to be calculated : the resistance $R_B$, the self-inductance $L_B$, the capacitance $C_B$ of the pickup loop and the mutual inductance between the resonator and the pickup loop $M_{DB}$. For the pickup loop with a square loop wire and a lumped capacitor, the first three properties are calculated by the same method introduced in previous section. The last property is calculated from electromagnetic theory as explained in the following subsection.

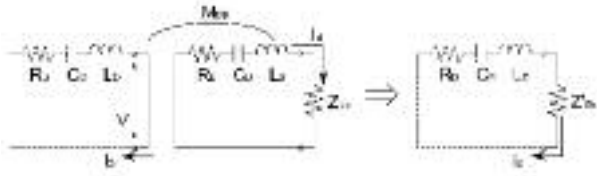

Fig. 10　Circuit model of the impedance transformation with pickup loop

### 5.2　Mutual inductance between square loops

For coupling of square loop wires, the theoretical formula of mutual inductance is derived from the Neumann formula (38), which expresses the mutual inductance of coupled circuits *s1* and *s2* in free space, as illustrated in **Fig. 11(a)**.

$$\frac{\mu_0}{4\pi}\int_{s_1}\int_{s_2}\frac{d\vec{s_1}\cdot d\vec{s_2}}{|\vec{s_1}-\vec{s_2}|} \tag{38}$$

Then the mutual inductance between two parallel wires of finite line, as shown in **Fig. 11(b),** is derived by using the Neumann formula as

$$M_{\parallel}(\ell_1,\ell_2,\xi,\zeta)=$$
$$m_{\parallel}(\ell_1,\ell_2,\xi,\zeta)+m_{\parallel}(\ell_1,\ell_2,-\xi,\zeta)-m_{\parallel}(\ell_1,-\ell_2,\xi,\zeta)-m_{\parallel}(\ell_1,-\ell_2,-\xi,\zeta) \tag{39}$$

The abbreviation *m* // is defined as

$$m_{\parallel}(\ell_1,\ell_2,\xi,\zeta)=$$
$$\frac{\mu_0}{8\pi}\left[(\ell_1+\ell_2+2\xi)\sinh^{-1}\frac{\ell_1+\ell_2+2\xi}{2\zeta}-\sqrt{(\ell_1+\ell_2+2\xi)^2+(2\zeta)^2}\right] \tag{40}$$

Now consider the couple of parallel square loop illustrated in **Fig. 11(c)**. The couple consists of 8 lines : line *a* to *d* and *A* to *D*. According to the Neumann formula, the mutual inductance of the couple is expressed by the summation of the mutual inductances among them.

$$M=\sum_{i=A,B,C,D}\sum_{j=a,b,c,d}M_{ij} \tag{41}$$

$M_{ij}$ represents the mutual inductance between the line *i* either of the line *A* to *D* and the line *j* either of the line *a* to *d*. The mutual inductances between the perpendicular lines such as $M_{ab}$ are all zero and those between the parallel lines including $M_{Aa}$ are expressed by using (39).

Hence the mutual inductance of the square loops is derived as

$$\begin{aligned}M=&M_{\parallel}\left[\ell_1,\ell_2,x,\sqrt{(\ell_-+y)^2+z^2}\right]-M_{\parallel}\left[\ell_1,\ell_2,x,\sqrt{(\ell_++y)^2+z^2}\right]\\&+M_{\parallel}\left[\ell_1,\ell_2,y,\sqrt{(\ell_--x)^2+z^2}\right]-M_{\parallel}\left[\ell_1,\ell_2,y,\sqrt{(\ell_+-x)^2+z^2}\right]\\&-M_{\parallel}\left[\ell_1,\ell_2,-x,\sqrt{(\ell_--y)^2+z^2}\right]-M_{\parallel}\left[\ell_1,\ell_2,-x,\sqrt{(\ell_+-y)^2+z^2}\right]\\&+M_{\parallel}\left[\ell_1,\ell_2,-y,\sqrt{(\ell_-+x)^2+z^2}\right]-M_{\parallel}\left[\ell_1,\ell_2,-y,\sqrt{(\ell_++x)^2+z^2}\right]\end{aligned} \tag{42}$$

Note that the abbreviation $\overline{\ell_\pm}$ is defined as

$$\overline{\ell_\pm}\equiv\frac{\ell_1\pm\ell_2}{2} \tag{43}$$

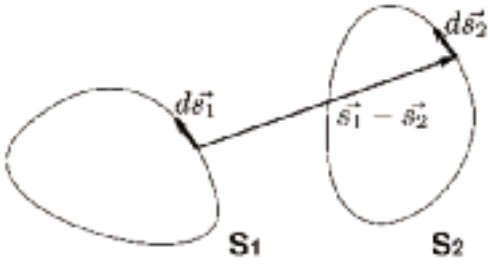


(a) Couple of circuits with uniform current distributions

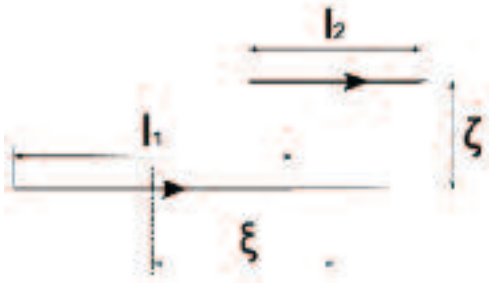


(b) Two parallel wires of finite line

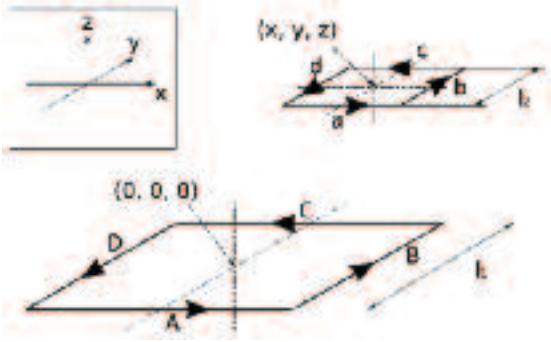


(c) Couple of parallel square loops

Fig. 11　Geometries applied for the Neumann formula to derive the mutual inductances

### 5.3　Experimental measurements

The measured wireless power transmission efficiencies with the three types of impedance ratio control are shown in **Fig. 12**. The theoretical curves are derived by using the measured coupling coefficient, quality factors and the theoretical formulas [14)-16)]. Note that the frequency of the power source is ,13.44 MHz, which is the average of the resonant frequency of the transmitting and receiving resonator.

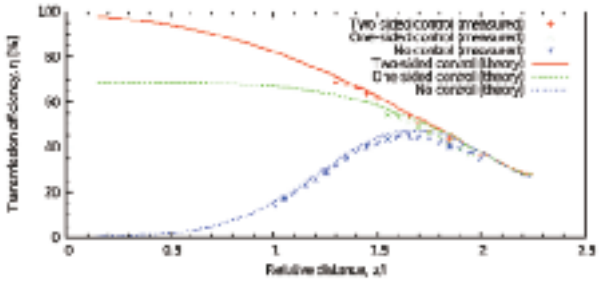

Fig. 12　Transmission efficiency with the three types of impedance matching control schemes. The relative distance is the ratio of a transmission distance $z$ = 200 - 400 mm and a side length $\ell$ = 198 mm of the transmitters and the receiver.

The measurement results of the pickup loop slide position are shown in **Fig. 13**. The theoretical, which means optimum, curve of the impedance ratio is derived by using the measured coupling coefficient, quality factors and the theoretical conditions of the impedance matching. The conditions are stated as (10) for the two-sided control and as (17) for the one-sided control. The measured value of the impedance ratio is estimated by using the measured pickup loop slide position and the theoretical formula of the impedance transformation (37) with the calculated properties of the resonator and the pickup loop.

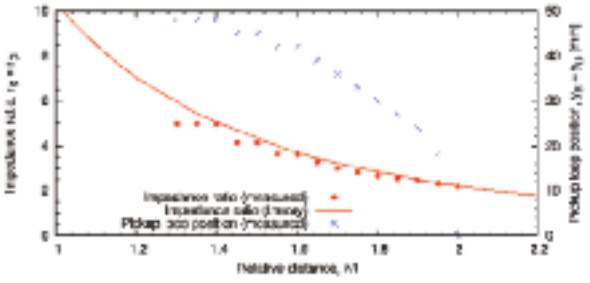

（a）Two-sided control

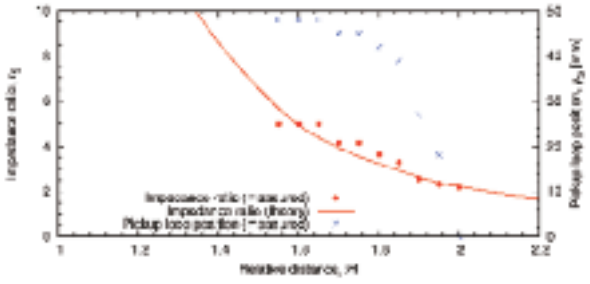

（b）One-sided control

Fig. 13　The impedance ratio and the pickup loop slide position

Each measured value well agreed with each theoretical value. Especially in the range of $z/\ell$ = 1.3-2.0 for the two-sided control, the wireless power transmission efficiency was as high as 30-70% even though the coupling coefficient is lower than 0.02. Hence the effectiveness of wireless power transmission with magnetic resonance was verified in the mid-range. The optimum pickup loop slide positions became smaller when the transmission distances got larger. In the result, the corresponding impedance ratios became smaller as the theory predicts. This is because the magnitude of the magnetic field inside the square loop is larger near the border and smaller near the center. The controllable transmission range is about $z/\ell$ = 1.3-2.0 with the two-sided control and $z/\ell$ = 1.5-2.0 with the one-sided control. The three efficiencies were equal at relative distance $z/\ell$ = 2.0. When the transmission distance became shorter, efficiency with the no control rapidly dropped. On the other hand, efficiency with the one-sided control went up a little and soon became almost constant.

These characteristics suggest a wireless power transmission system with magnetic resonance will have to carefully choose a proper impedance matching control scheme according to the moving range of mobile receivers in practical use. In narrow transmission distance range, no control would be enough. But in wide transmission distance range, one-sided control is needed at least. If the application needs much higher efficiency at shorter distances, the two-sided control should be implemented.

## 6. Conclusions

This chapter studied the feasibility of wireless power transmission with magnetic resonance to mobile objects.

The theory of magnetic resonance was analyzed not with the coupled-mode theory but with the electrical engineering theory to emphasize the essential elements of magnetic resonance : high quality factor resonator and impedance matching system. The theory also derives the three schemes of impedance matching control. Two-sided control produces the maximum efficiency while it would require higher hardware and software costs. No control will only need a simple and low-cost system in exchange for efficiency at various transmission distances. One-sided control has middle characteristics between the first two.

A transmitter and receiver system prototype was developed to verify the theory and to discuss the realizable performance of a compactly-implemented resonator and impedance matching system. The resonator was a loop with capacitor type resonator and the impedance matching system was a sliding pickup loop system.

Evaluation of the resonator quality factor showed the loop with capacitor type resonator had a higher quality factor than the other compactly-shaped dense coil type resonator. And it was proven that the quality factor depends not only on radiation and ohmic loss but also on capacitor loss.

The theoretical analysis of the sliding pickup loop system and the power transmission experiment were explained. It showed that the couple of the pickup loop and the resonator functions as an inductive transformer and the sliding position of the pickup loop controls the impedance ratio. The power transmission experiment also verified the theory of wireless power transmission with magnetic resonance and the theoretical characteristics of tree impedance matching control schemes.

## References


1) A. Karalis, J. D. Joannopoulos and M. Soljačić : “Efficient wireless non-radiative mid-range energy transfer”, Annals of Physics, Volume 323 (2008), Issue 1, pp. 34-48.
2) A. Kurs, A. Karalis, R. Moffatt, J. D. Joannopoulos, P. Fisher and M. Soljačić : ”Wireless Power Transfer via Strongly Coupled Magnetic Resonances”, Science Magazine, Volume 317(No. 5834) (2007), pp. 83-86.
3) Carl T.A. Johnk : “Engineering Electromagnetic Fields and Waves”, Wiley (1975)
4) D. M. Pozer : “Microwave Engineering, 2nd ed.”, Wiley (1998)
5) Frederick Warren Grover : “Inductance Calculations : Working Formulas and Tables”, Van Nostrand (1946)
6) H. Ayano, H. Nagase and H. Inaba : “High Efficient Contactless Electrical Energy Transmission System”, IEEJ Tran. IA, Volume 123(No. 3) (2003), pp. 263-270.
7) T. Komaru, M. Koizumi, K. Komurasaki, T. Shibata and K. Kano : “Parametric Evaluation of Mid-range Wireless Power Transmission with Magnetic Resonance”, Proceedings of the IEEE-ICIT 2010 International Conference on Industrial Technology (2010), pp.789-792.
8) N. Ehara, Y. Nagatsuka, Y. Kaneko, S. Abe, T. Yasuda and K. Ida : “Compact and Rectangular Transformer of Contactless Power Transfer System for Electric Vehicle, The Papers of Technical Meeting on Vehicle Technology (2007), pp.7-12.

## ＜著　者＞


小丸　　尭
（こまる　たかし）
研究開発3部
無線通信，無線電力の研究に
従事

小泉　正剛
（こいずみ　まさよし）
パナソニック株式会社
※当該研究は東京大学大学院
在学時に従事したもの

小紫　公也
（こむらさき　きみや）
東京大学大学院工学系研究科
航空宇宙工学専攻教授
博士（工学）
無線電力伝送，将来型宇宙推進
システム，高温プラズマ・レー
ザー応用の研究に従事

柴田　貴行
（しばた　たかゆき）
基礎研究3部
高周波集積回路，センサ回路の
研究に従事

加納　一彦
（かのう　かずひこ）
基礎研究2部
MEMS技術，ナノカーボン材料
を用いた自動車用センサ・アク
チュエータの研究開発に従事